JCB Article

ROCK and mDia1 antagonize in Rho-dependent Rac activation in Swiss 3T3 fibroblasts

Takahiro Tsuji,[1] Toshimasa Ishizaki,[1] Muneo Okamoto,[1] Chiharu Higashida,[1] Kazuhiro Kimura,[1] Tomoyuki Furuyashiki,[1] Yoshiki Arakawa,[1] Raymond B. Birge,[2] Tetsuya Nakamoto,[3] Hisamaru Hirai,[3] and Shuh Narumiya[1]

[1]Department of Pharmacology, Kyoto University Faculty of Medicine, Kyoto 606-8501, Japan
[2]Department of Biochemistry and Molecular Biology, University of Medicine and Dentistry of New Jersey, New Jersey Medical School, NJ 07214
[3]Department of Hematology and Oncology, Faculty of Medicine, University of Tokyo, Tokyo 113-8655, Japan

The small GTPase Rho acts on two effectors, ROCK and mDia1, and induces stress fibers and focal adhesions. However, how ROCK and mDia1 individually regulate signals and dynamics of these structures remains unknown. We stimulated serum-starved Swiss 3T3 fibroblasts with LPA and compared the effects of C3 exoenzyme, a Rho inhibitor, with those of Y-27632, a ROCK inhibitor. Y-27632 treatment suppressed LPA-induced formation of stress fibers and focal adhesions as did C3 exoenzyme but induced membrane ruffles and focal complexes, which were absent in the C3 exoenzyme-treated cells. This phenotype was suppressed by expression of N17Rac. Consistently, the amount of GTP-Rac increased significantly by Y-27632 in LPA-stimulated cells. Biochemically, Y-27632 suppressed tyrosine phosphorylation of paxillin and focal adhesion kinase and not that of Cas. Inhibition of Cas phosphorylation with PP1 or expression of a dominant negative Cas mutant inhibited Y-27632–induced membrane ruffle formation. Moreover, Crk-II mutants lacking in binding to either phosphorylated Cas or DOCK180 suppressed the Y-27632–induced membrane ruffle formation. Finally, expression of a dominant negative mDia1 mutant also inhibited the membrane ruffle formation by Y-27632. Thus, these results have revealed the Rho-dependent Rac activation signaling that is mediated by mDia1 through Cas phosphorylation and antagonized by the action of ROCK.

Introduction

Cells adopt different shapes in response to different stimuli. For example, interphase nonmotile Swiss 3T3 fibroblasts extend filopodia or lamellipodia or form stress fibers and focal adhesions in response to bradykinin, PDGF, and lysophosphatidic acid (LPA),* respectively, and these changes are mediated respectively by the Rho family small GTPases, Cdc42, Rac, and Rho (Hall, 1998). Migrating fibroblasts also exhibit lamellipodia, filopodia, and actin bundles with focal adhesions. However, in these cells those structures are observed in different places of a single cell. Filopodia and lamellipodia are seen in the leading edge of the cell, actin bundles similar to stress fibers are running from the front to the rear, and focal adhesions are at the tips of these bundles (Mitchison and Cramer, 1996; Horwitz and Parsons, 1999). It is also noteworthy that these structures change in space as the cell migrates. There is accumulating evidence that the Rho family small GTPases participate also in these shape changes of migrating cells (Allen et al., 1998; Nobes and Hall, 1999). However, how the activities of these GTPases are regulated spatiotemporally in migrating cells remains largely unknown.

The actions of the Rho GTPases are mediated by the respective groups of downstream effectors (Schmitz et al., 2000). Using the selective binding to the GTP-bound active form of Rho, several effectors of Rho were isolated (Narumiya, 1996). Among them, the ROCK–ROK–Rho kinase family of serine-threoine protein kinases has been found essential in Rho-induced formation of stress fibers and focal adhesions. Expression of a dominant negative form of this kinase or the addition of a specific inhibitor of this kinase Y-27632 inhibits stress fibers and focal adhesions induced by LPA or activated Rho in several cell lines (Ishizaki et al., 1997; Uehata et al.,

Address correspondence to Shuh Narumiya, Dept. of Pharmacology, Kyoto University Faculty of Medicine, Yoshida, Sakyo-ku, Kyoto 606-8501, Japan. Tel.: 81-75-753-4392. Fax: 81-75-753-4693. E-mail: snaru@mfour.med.kyoto-u.ac.jp

*Abbreviations used in this paper: FAK, focal adhesion kinase; GAP, GTPase-activating protein; GFP, green fluorescent protein; GST, glutathione *S*-transferase; LPA, lysophosphatidic acid; MT, microtubule.

Key words: Rho; mDia; Rac; membrane ruffles; Y-27632

1997). However, expression of a dominant active ROCK mutant alone leads to the formation of an aberrant form of centrally contracted actin bundles in the cell (Leung et al., 1996; Amano et al., 1997; Ishizaki et al., 1997), indicating that other Rho effector(s) cooperate to induce well-aligned stress fibers. We found recently that coexpression of an active mutant of another Rho effector, mDia1, corrected the alignment of actin bundles induced by active ROCK (Watanabe et al., 1999). Our subsequent study indicates that this mDia1 action is exerted through its action on microtubule (MT) alignment (Ishizaki et al., 2001). The structures of the actin cytoskeleton induced by ROCK and mDia1 reflect the pattern and location of focal adhesions induced by each of them. Dominant active ROCK mutants induce abnormally large adhesions not only in the cell periphery but also in the center of the cells. On the other hand, expression of active mDia1 mutants induces small adhesions at the tips of the cell. Theses results suggest that ROCK and mDia differently regulate shapes and locations of focal adhesions. However, how these two molecules affect signals and dynamics of focal adhesions remains unknown. There are several studies suggesting the regulation, by multiple Rho effector(s), of the processes involving the cell to substrate adhesion. For example, Nobes and Hall (1999) examined effects of C3 exoenzyme and Y-27632 on REF cells subjected to the in vitro wound healing assay and found that the C3 exoenzyme treatment abolished the cell migration, whereas Y-27632 stimulated it. Y-27632 was also reported not to block the G1 to S phase progression of the cell cycle in Swiss 3T3 cells (Ishizaki et al., 2000), which is sensitive to the C3 exoenzyme treatment (Yamamoto et al., 1993).

In this study, we compared the effects of C3 exoenzyme with those of Y-27632 first morphologically on rearrangement of actin cytoskeleton and focal adhesion and then biochemically on tyrosine phosphorylation of focal adhesion proteins. We also tested the effects of overexpression of several signaling molecules and inhibitors of Src and MT dynamics on the elicitation of the phenotype induced by ROCK inhibition. Our findings show that there is a dichotomy of the signaling from Rho, one being mediated by ROCK leading to tyrosine phosphorylation of focal adhesion kinase (FAK) and paxillin and the other mediated by mDia1 resulting in phosphorylation of Cas, and that the latter mDia1 pathway leads to activation of Rac, which is antagonistically regulated by the former ROCK pathway.

Results

Different effects of C3 exoenzyme and Y-27632 on LPA-induced actin reorganization and formation of focal adhesions in Swiss 3T3 cells

We stimulated serum-starved Swiss 3T3 fibroblasts with LPA and examined the effects of C3 exoenzyme that shuts off all of the Rho signals and those of Y-27632 that selectively inhibit ROCK-mediated pathway downstream of Rho. We first assessed their effects on actin cytoskeleton and focal adhesions by staining cells with phalloidin and antiphosphotyrosine antibody, respectively (Fig. 1 A). As originally shown by Ridley and Hall (1992), LPA addition to serum-starved 3T3 cells spread the cells and induced stress fibers and focal adhesions in a few minutes, and this change was completely inhibited by prior C3 exoenzyme treatment. The C3 exoenzyme-treated cells remained round with many beaded processes. On the other hand, the addition of Y-27632 did not affect the morphology of serum-starved cells, and when LPA was added to these cells they flattened and spread as seen in control cells. However, they did not develop actin stress fibers, but a thick rim of F-actin accumulation was seen in the cell periphery. Simultaneous staining with antiphosphotyrosine showed numerous small dot-like structures beneath this F-actin accumulation, which resembled Rac-induced focal complexes. Video microscopy revealed that LPA addition evoked robust membrane ruffles in the periphery of the Y-27632–treated cells (Fig. 1 B), suggesting that the thick actin rim detected by phalloidin staining represents membrane ruffles. We examined the specificity of this Y-27632 effect by two additional experiments. First, the addition of Y-27632 to the C3 exoenzyme-treated cells did not evoke LPA-induced cell spreading and membrane ruffles (Fig. S1 available at http://www.jcb.org/cgi/content/full/jcb.200112107/DC1). Second, the addition of PDGF could induce membrane ruffles in the C3 exoenzyme-treated cells (Fig. S2 available at http://www.jcb.org/cgi/content/full/jcb.200112107/DC1). These results indicate that the membrane ruffles seen in the Y-27632–treated cells occur in a Rho-dependent, ROCK-independent manner.

Rac is activated by a Rho-dependent, ROCK-independent signaling

Because membrane ruffles are usually induced by Rac activation, we suspected that Rac is activated under the above conditions and induces membrane ruffles in the Y-27632–treated cells. Therefore, we transfected Swiss 3T3 cells with dominant negative Rac (N17Rac) and examined the effect of its expression on the LPA-induced membrane ruffling in Y-27632–treated cells. As shown in Fig. 2 A, the cells expressing N17Rac showed no rim-like accumulation of F-actin in the periphery, and F-actin dispersed in the cytoplasm. Thin F-actin spikes were also seen around the cell periphery. These cells did not show dot-like accumulation of antiphosphotyrosine staining in the cell periphery either, and anti-phosphotyrosine staining accumulated in the cytoplasm as seen in C3 exoenzyme-treated cells. This phenotype was observed in 200 cells in a total of 235 cells observed in three independent experiments. These results suggest that activation of Rac occurred in the Y-27632–treated cells upon LPA addition and was responsible for membrane ruffle formation. To confirm this hypothesis biochemically, we performed the pull-down assay for GTP-Rac using a glutathione *S*-transferase (GST) fusion of the CRIB domain of Pak (Sander et al., 1998). As shown in Fig. 2 B, virtually no GTP-Rac was pulled down from lysates of any groups of serum-starved cells tested. A small but significant amount of GTP-Rac was precipitated from the lysates of the control cells stimulated with LPA. The precipitation of GTP-Rac was significantly enhanced in the Y-27632–treated cells stimulated with LPA and not in the C3 exoenzyme-treated cells. These results verified that Rac was activated in the Y-27632–treated cells upon LPA addition and suggest that this activation is induced by the Rho-dependent, ROCK-independent signaling.

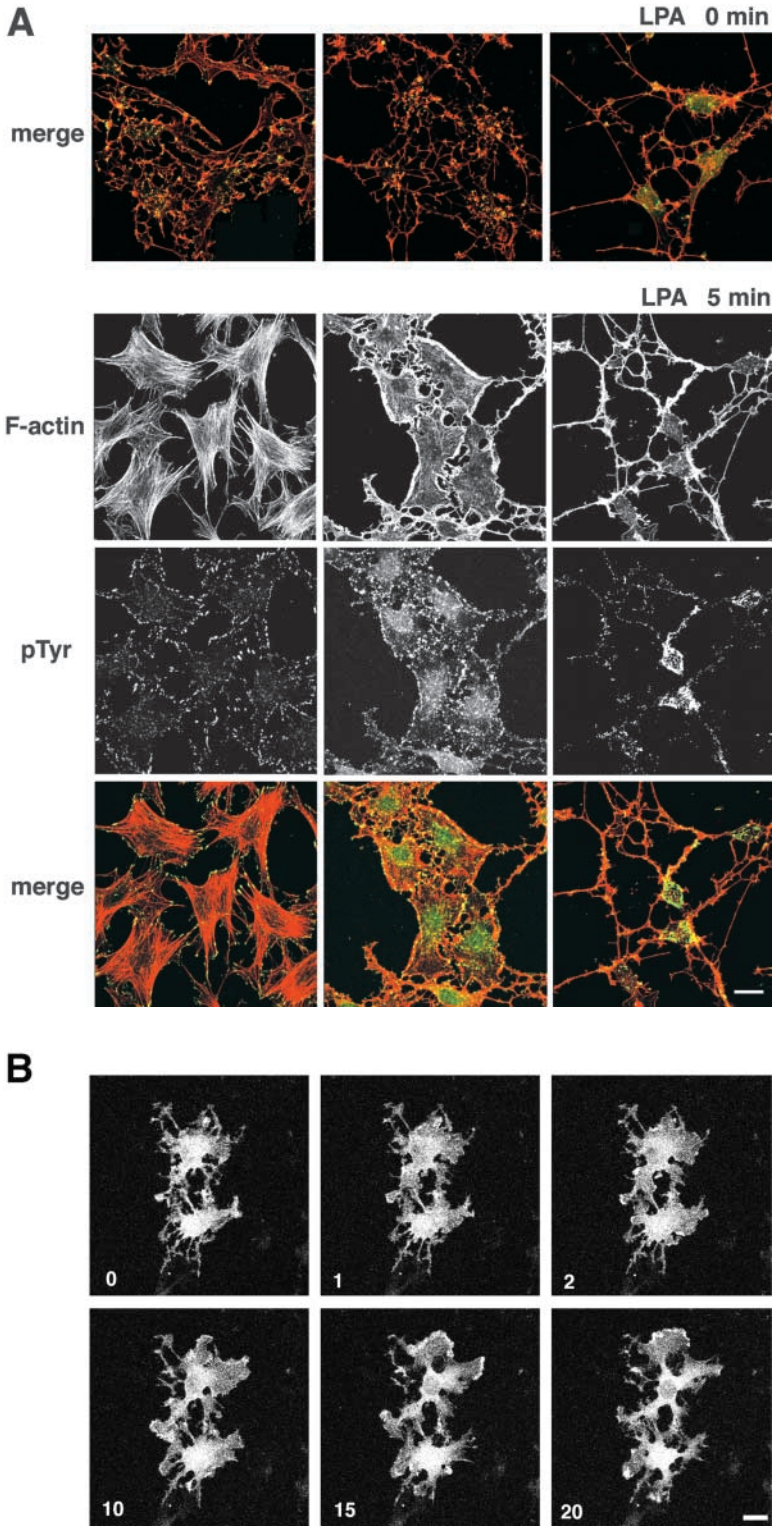

Figure 1. **Effects of C3 exoenzyme and Y-27632 on actin reorganization and localization of tyrosine-phosphorylated proteins in LPA-stimulated Swiss 3T3 cells.** (A) Immunofluorescence. Swiss 3T3 cells were maintained in DME containing 10% FBS for 3 d and cultured in serum-free DME for 24 h. During this period, the cells were without any treatment or treated with either 30 μg/ml C3 exoenzyme for 4 d or with 30 μM Y-27632 for 30 min and then exposed to 5 μM LPA for 0 and 5 min. The cells were fixed, permeabilized, and stained with Texas red phalloidin for F-actin (red) and antiphosphotyrosine antibody (green). The top panels show the merged images of the cells without LPA stimulation. The F-actin staining, the phosphotyrosine staining, and the merged images of the LPA-stimulated cells are shown in the second, third, and the bottom rows of the panels, respectively. Note that the cells treated with Y-27632 display a thick rim of F-actin and dot-like phosphotyrosine staining in the cell periphery upon the addition of LPA. (B) Video microscopy. Swiss 3T3 cells transfected with GFP actin were serum starved for 24 h and treated with 30 μM Y-27632 for the last 30 min. LPA was added at 5 μM, and the cell shape change was monitored in the continued presence of Y-27632 by time-lapse confocal microscopy as the image of GFP actin. The number in each image indicates time after the LPA addition in min. See also the video available at http://www.jcb.org/cgi/content/full/jcb.200112107/DC1. Bars, 20 μm.

Tyrosine phosphorylation of p130Cas occurs through the Rho-dependent, ROCK-independent signaling

To elucidate the above Rho-dependent, ROCK-independent signaling biochemically, we compared the effects of C3 exoenzyme and Y-27632 on LPA-induced tyrosine phosphorylation of focal adhesion proteins. Swiss 3T3 cells were treated with either vehicle, C3 exoenzyme, or Y-27632 for the indicated times and then stimulated with LPA for 0, 5, and 30 min. Cell lysates were prepared and subjected to immunoblotting and immunoprecipitation analysis. As shown in Fig. 3 A, LPA addition induced tyrosine phosphorylation of proteins of ~70 and 120–130 kD, which correspond to a group of phosphorylated paxillin isoforms and a combined band of p125FAK and p130Cas, respectively. The C3 exoenzyme treatment suppressed tyrosine phosphorylation of both groups of proteins as reported previously (Kumagai et

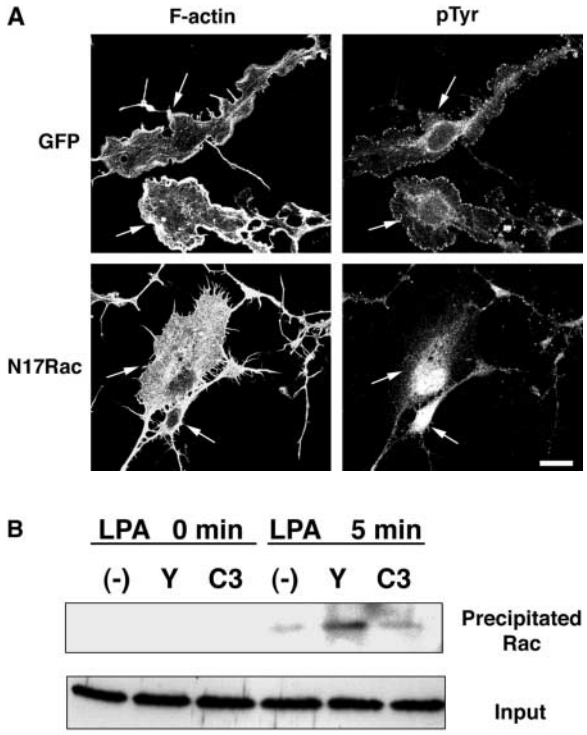

Figure 2. **LPA-induced Rac activation in Y-27632–treated Swiss 3T3 cells.** (A) Inhibition of membrane ruffles by expression of N17Rac in Y-27632–treated cells. Swiss 3T3 cells were transfected with 1 μg of pCMV5–N17Rac or 1 μg of pEGFP–C1. The transfected cells were cultured in DME containing 10% FBS for 16 h and then in serum-free DME for 24 h. The cells were treated with 30 μM Y-27632 for 30 min and then stimulated with LPA for 5 min. The cells were stained for F-actin and phosphotyrosine as described in the legend to Fig. 1. Arrows indicate transfected cells identified with anti-GFP (top) or anti-Flag staining (bottom). Note that membrane ruffles and focal complexes disappeared in the cells overexpressing N17Rac. Bar, 20 μm. (B) Pull-down assay for GTP-Rac. Swiss 3T3 cells were cultured and treated with either C3 exoenzyme or Y-27632 as described in the legend to Fig. 1. The cells were then stimulated with 5 μM LPA for 0 and 5 min and subjected to the pull-down assay as described in Materials and methods. GTP-Rac precipitated from each cell lysates was analyzed by immunoblotting with anti-Rac antibody (top), and the total amounts of Rac present in the cell lysates are shown in the immunoblot in the bottom panels. −, cells without any pretreatment; Y, cells treated with Y-27632; C3, cells treated with C3 exoenzyme. Note that GTP-Rac increased in amount significantly by Y-27632 treatment and remained little in the C3 exoenzyme-treated cells.

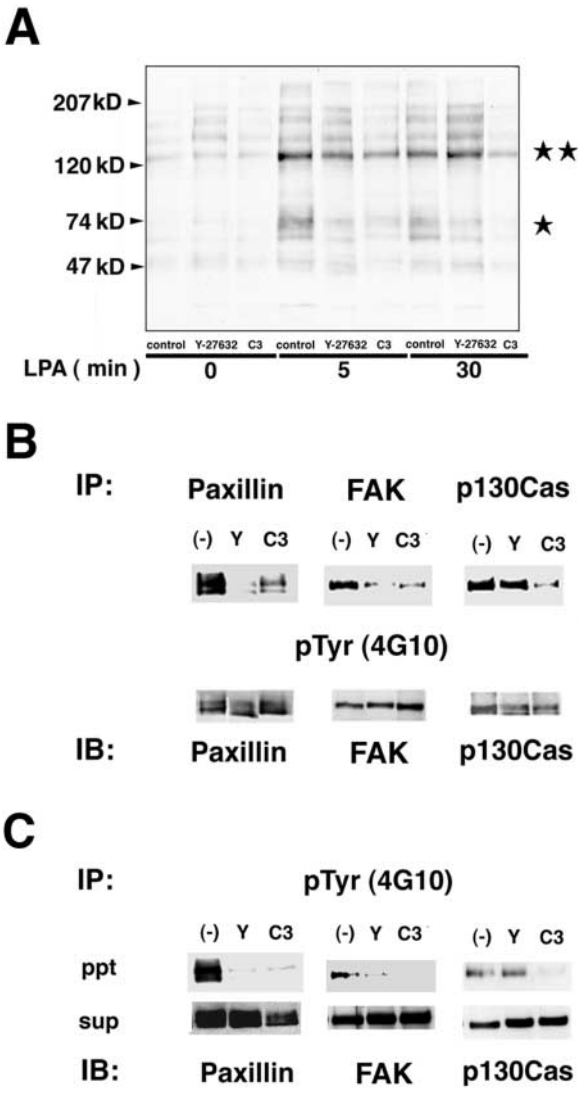

Figure 3. **Different effects of C3 exoenzyme and Y-27632 on tyrosine phosphorylation of focal adhesion proteins.** (A) Effects of C3 exoenzyme and Y-27632 on LPA-induced tyrosine phosphorylation. Swiss 3T3 cells were cultured and treated either with none, C3 exoenzyme, or Y-27632 as described in the legend to Fig. 1. The cells were then stimulated with 5 μM LPA for 0, 5, and 30 min. The cell lysates were prepared and subjected to SDS-PAGE and immunoblotting using antiphosphotyrosine antibody. A single asterisk and double asterisk indicate the tyrosine-phosphorylated paxillin isoforms and the combined band of phosphorylated FAK and Cas, respectively. (B and C) Inhibition of tyrosine phosphorylation of FAK and paxillin but not that of Cas by Y-27632 treatment. The lysates of cells stimulated with LPA for 5 min were subjected to immunoprecipitation using either antipaxillin, anti-FAK, or anti-p130Cas antibodies (B) or using antiphosphotyrosine antibody (C). The immunoprecipitates were then analyzed by immunoblotting with antiphosphotyrosine antibody (B) or with antipaxillin, anti-FAK, and anti-p130Cas antibodies (C). −, cells without any pretreatment; Y, cells treated with Y-27632; C3, cells treated with C3 exoenzyme. Note that Y-27632 treatment suppressed tyrosine phosphorylation of paxillin and FAK but not that of Cas, whereas the phosphorylation of these three proteins were equally suppressed by C3 exoenzyme treatment.

al., 1993; Rankin et al., 1994; Needham and Rozengurt, 1998). On the other hand, Y-27632 suppressed tyrosine phosphorylation of the 70-kD group but only partially affected that of the 120–130-kD group. The tyrosine phosphorylation of the latter group declined at 30 min in the control cells, whereas it remained high in the Y-27632–treated cells. Immunoprecipitation experiments using antipaxillin, anti-FAK, and anti-Cas antibodies revealed that Y-27632 treatment suppressed tyrosine phosphorylation of paxillin and FAK to the extent similar to that achieved by C3 exoenzyme treatment, whereas it barely inhibited the phosphorylation of Cas (Fig. 3 B). The same result was obtained by immunoblotting with antipaxillin, anti-FAK, and anti-Cas antibodies of proteins precipitated with antiphosphotyrosine monoclonal antibody (Fig. 3 C). These results suggest the presence of a dichotomy of the signaling from Rho to the tyrosine phosphorylation of focal adhesion pro-

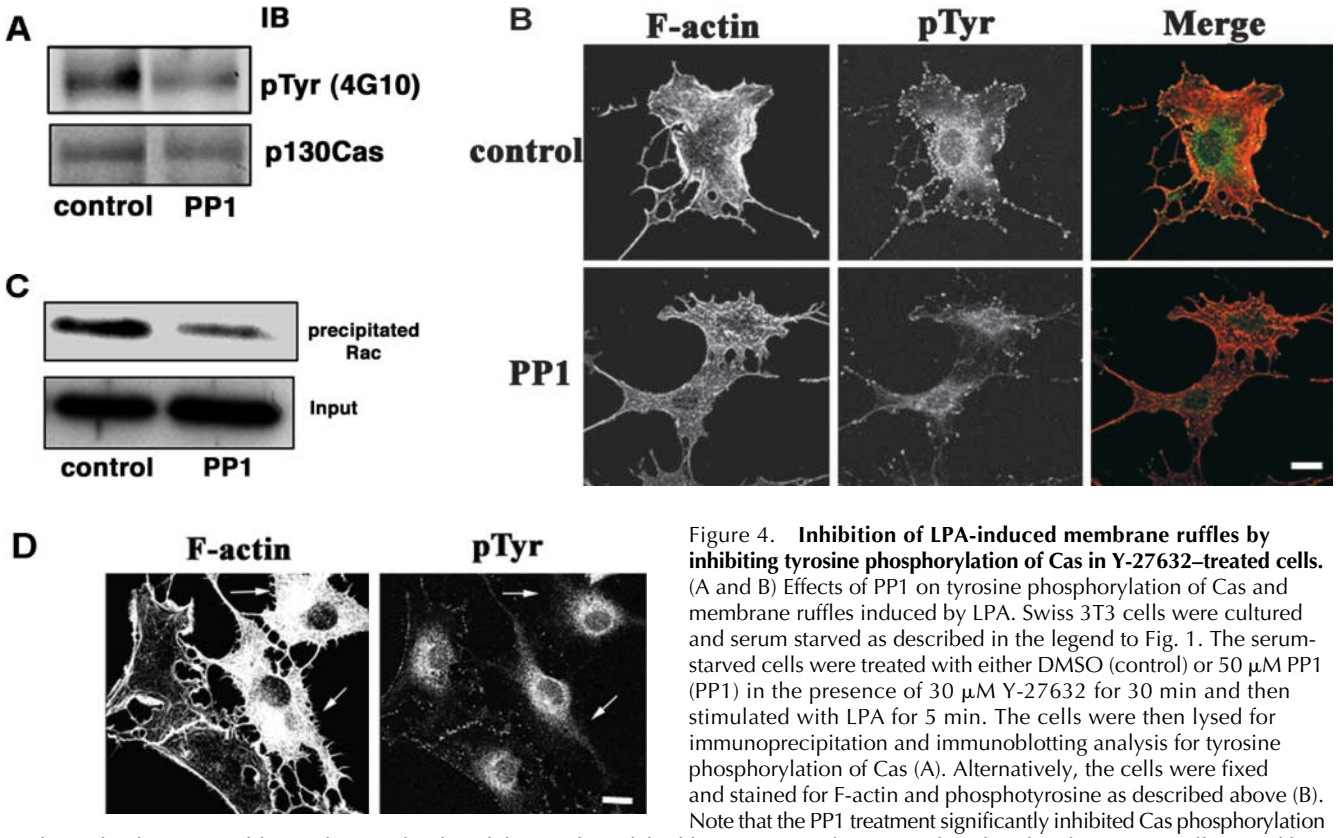

Figure 4. **Inhibition of LPA-induced membrane ruffles by inhibiting tyrosine phosphorylation of Cas in Y-27632–treated cells.** (A and B) Effects of PP1 on tyrosine phosphorylation of Cas and membrane ruffles induced by LPA. Swiss 3T3 cells were cultured and serum starved as described in the legend to Fig. 1. The serum-starved cells were treated with either DMSO (control) or 50 μM PP1 (PP1) in the presence of 30 μM Y-27632 for 30 min and then stimulated with LPA for 5 min. The cells were then lysed for immunoprecipitation and immunoblotting analysis for tyrosine phosphorylation of Cas (A). Alternatively, the cells were fixed and stained for F-actin and phosphotyrosine as described above (B). Note that the PP1 treatment significantly inhibited Cas phosphorylation as shown by the immunoblot analysis and reduced the number of dot-like structures of tyrosine-phosphorylated proteins as illustrated by antiphosphotyrosine staining. Significant suppression of membrane ruffles is also noted in the PP1-treated cells. (C) Effects of PP1 on the level of GTP-Rac in Y-27632–treated cells. The cells were cultured and treated as described above and then subjected to the pull-down assay for GTP-Rac. Control, cells treated with Y-27632 alone; PP1, cells treated with both Y-27632 and PP1. (D) Inhibition of LPA-induced membrane ruffles by expression of CasΔSD, a tyrosine phosphorylation-defective Cas mutant, in Y-27632–treated cells. Swiss 3T3 cells were transfected with 1 μg of pSSRα–CasΔSD and cultured as described in the legend to Fig. 2 A. The cells were then treated with 30 μM Y-27632 for 30 min and stimulated with 5 μM LPA for 5 min in the continued presence of Y-27632. The cells were fixed, and F-actin and tyrosine-phosphorylated proteins were stained as described above. The cells expressing CasΔSD were identified by HA tag staining and are indicated by arrows. Bars, 20 μm.

teins; one is mediated by ROCK and induces the phosphorylation of paxillin and FAK, and the other is ROCK independent and leads to the phosphorylation of Cas.

Tyrosine phosphorylation of Cas is required for LPA-induced membrane ruffling in Y-27632–treated cells

As previously reported (Sakai et al., 1994; Klinghoffer et al., 1999), p130Cas was tyrosine phosphorylated by the Src family of kinases. Therefore, we examined LPA-induced changes in Y-27632–treated cells in the presence of PP1, a specific inhibitor of Src family kinases (Hanke et al., 1996). Consistent with the previous report (Okuda et al., 1999), the treatment with PP1 significantly decreased the level of tyrosine phosphorylation of Cas (Fig. 4 A). Under these conditions, LPA-induced morphological changes were also inhibited (Fig. 4 B). The peripheral accumulation of F-actin was greatly suppressed, and F-actin was seen as disorganized tangles in the cytoplasm. Focal complexes beneath the membrane ruffles disappeared. These changes were observed in almost all PP1-treated cells. We also used the pull-down assay and have found that the level of GTP-Rac was significantly suppressed by the PP1 treatment (Fig. 4 C). These results suggest that the Cas phosphorylation leads to Rac activation and evokes membrane ruffles. To confirm this, we transfected 3T3 cells with CasΔSD. CasΔSD is a Cas mutant with a deletion of the tyrosine phosphorylation sites by Src kinase (Nakamoto et al., 1997), and overexpression of this mutant works as a dominant negative form in Cas signaling involving the phosphorylation (Klemke et al., 1998). As shown in Fig. 4 D, no LPA-induced membrane ruffling was seen, and the dot-like focal complexes disappeared in the Y-27632–treated cells expressing CasΔSD. F-actin was dispersed in the cytoplasm as observed in the cells expressing RacN17 (Fig. 2 A). This phenotype was observed in 48 cells out of 50 Cas‴ ΔSD-expressing cells in three independent experiments.

Overexpression of CrkII(R38K) and CrkII(W170K) inhibits LPA-induced membrane ruffling in Y-27632–treated cells

Tyrosine phosphorylation of Cas provides a binding site for Crk, which then binds DOCK180 to make a Cas–Crk–DOCK180 complex (O'Neill et al., 2000). Because DOCK180 is known as an activator for Rac (Kiyokawa et al., 1998), we examined the involvement of this complex formation in LPA-induced ruffling in our system. To this

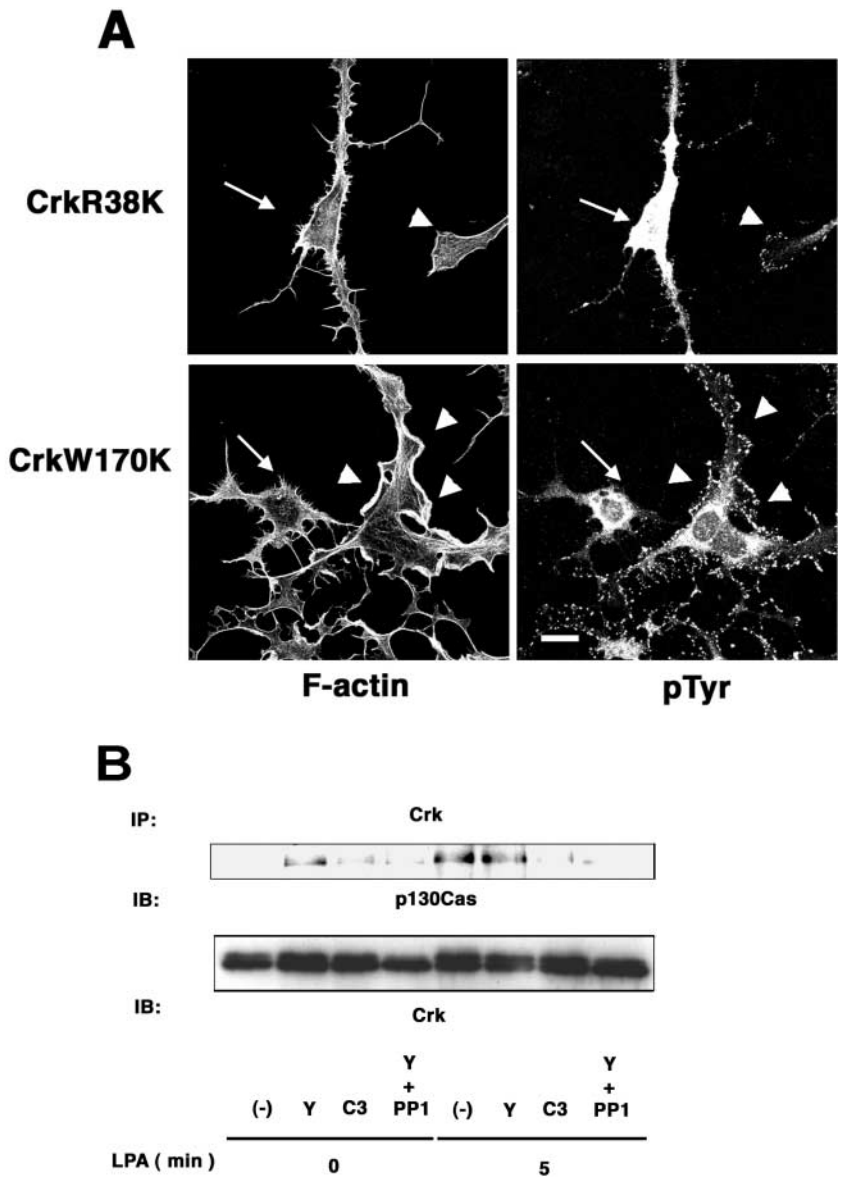

Figure 5. **Cas–Crk interaction in LPA-induced membrane ruffles in Y-27632–treated cells.** (A) Inhibition of the ruffle formation by expression of CrkII mutants. The cells were transfected either with 1 μg of pEEB–CrkII(R38K) and 0.1 μg of pEGFP–C1 (top) or with 1 μg of pEEB–CrkII(W170K) and 0.1 μg of pEGFP–C1 (bottom) and cultured as described in the legend to Fig. 2 A. The cells were then treated with 30 μM Y-27632 for 30 min and stimulated with 5 μM LPA for 5 min in the continued presence of Y-27632. The cells were fixed, and F-actin and tyrosine-phosphorylated proteins were stained as described above. The cells expressing each CrkII mutant were identified with anti-GFP staining and are indicated by arrows. Arrowheads indicate nontransfected cells. Note that the cell bodies of the cells expressing these CrkII mutants retracted, and the dot-like structure of tyrosine-phosphorylated proteins disappeared in the cell periphery. Bar, 20 μm. (B) Rho-dependent formation of the Cas–Crk complex in LPA-stimulated cells. Swiss 3T3 cells were cultured and treated with indicated reagents as described in the legends for Figs. 1 and 4. After stimulated with LPA for 0 and 5 min, the cells were lysed and subjected to immunoprecipitation with anti-Crk mAb. The immunoprecipitates were then analyzed by Western blot analysis with anti-Cas antibody.

purpose, we used two CrkII mutants. One is CrkII(R38K) that has a mutation in its SH2 region and is devoid of binding to Cas, and the other is CrkII(W170K) that has a mutation in its NH_2-terminal SH3 region and is devoid of binding to DOCK180 (Albert et al., 2000). Overexpression of either of the two mutants significantly blunted the LPA-induced responses in Y-27632–treated cells. The cells expressing the CrkII mutants did not spread and did not develop membrane ruffling (Fig. 5 A). The dot-like staining with antiphosphotyrosine antibody was not seen either in the cell periphery. Suppression of the membrane ruffles was found in all of the 20 CrkII(R38K) cells and 23 out of 24 CrkII(W170K) cells observed in three independent experiments. Together, these results suggest that Rac activation through Rho-dependent, ROCK-independent pathway in LPA-stimulated cells is mediated through Cas phosphorylation and the induction of the Cas–Crk–DOCK180 complex. Consistently, the Cas–Crk complex was formed in LPA-stimulated cells, and this formation was inhibited by treatment with either C3 exoenzyme or PP1 (Fig. 5 B).

Effects of mDia1 mutants on LPA-induced membrane ruffling in Y-27632–treated cells

The next question is the identity of the Rho effector mediating the Rho signaling to Cas phosphorylation. An obvious candidate is mDia1 because mDia1 cooperates with ROCK to induce stress fibers and focal adhesions (Watanabe et al., 1999). The interaction of mDia with Src was also reported (Tominaga et al., 2000). To identify the involvement of mDia1, we first prepared several truncation constructs of mDia1ΔN3. mDia1ΔN3 is a dominant active mutant that induces thin stress fibers and small focal adhesions in HeLa cells (Watanabe et al., 1999; Ishizaki et al., 2001). Mutants interfering with this phenotype are, therefore, expected to work as dominant negative forms in cells in physiological situations. Because mDia1ΔN3 consists of several domains and deletion of any of these domains leads to the loss of the active phenotype, we suspected that truncation mutants of this active mutant might compete with the full mDia1ΔN3 and interfere with its action. To test this possibility, we made mutants H + P, F2, CC, and mDia1ΔN3(HindIII) (Fig. 6 A). Among these mu-

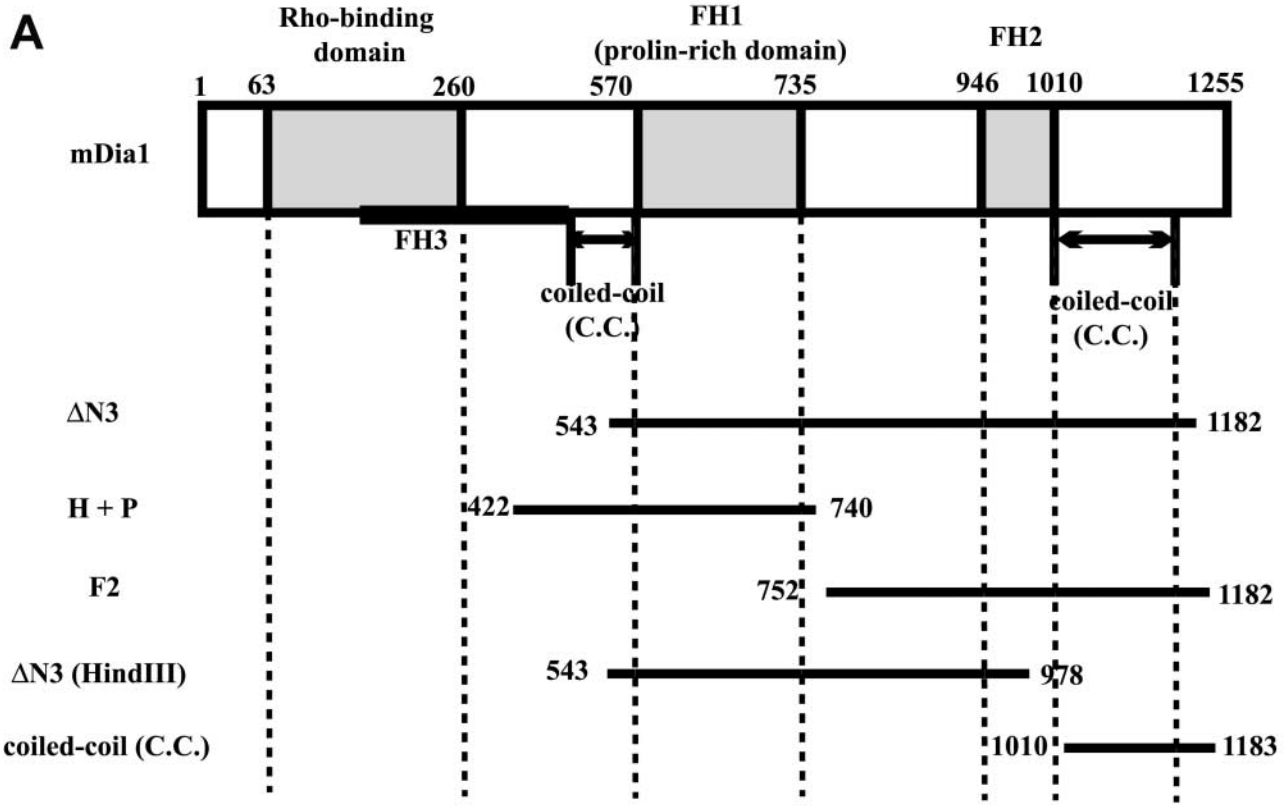

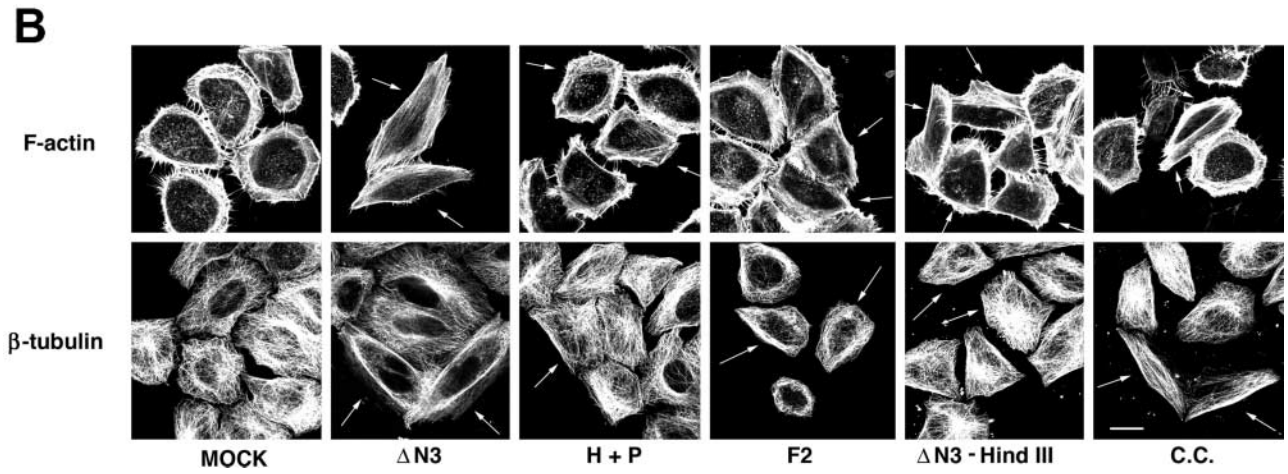

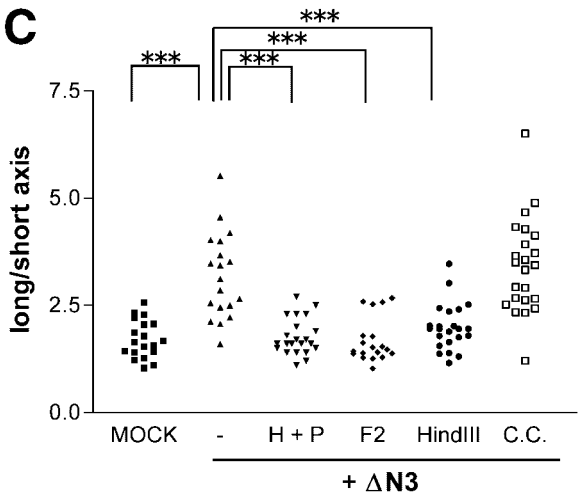

Figure 6. **Effects of various mDia1 fragments on the mDia1ΔN3 phenotype in HeLa cells.** (A) Schematic diagram of the structures of mDia1 and truncation mutants. The domain structure of mDia1 is shown above. The Rho-binding domain and the FH1 and FH2 regions are shown by hatched boxes. The FH3 region that partially overlaps with the Rho-binding domain and the two coiled-coil regions are indicated by a thick line and two-headed arrows, respectively. Truncation mutants, ΔN3, H + P, F2. ΔN3(HindIII) and CC are shown by the lines below. Numbers indicate the amino acid number at the NH_2 and COOH terminals of each protein and domain. (B and C) Effects of various fragments on the mDia1ΔN3 phenotype. HeLa cells were transfected with 0.2 μg of pFL–mDia1ΔN3 either alone or with 2 μg of pEGFP plasmid encoding either mDia1 H + P, F2, ΔN3(HindIII), or CC mutant. After the culture for 24 h, the cells were fixed and stained for F-actin (top) and β-tubulin (bottom) (B). Arrows indicate the cells expressing each construct. The ratios of the long versus short axis were measured in the cells expressing each construct and are shown (C). Note that expression of either H + P, F2, or ΔN3(HindIII) inhibits the cell elongation and the parallel alignment of F-actin bundles and MTs induced by mDia1ΔN3.

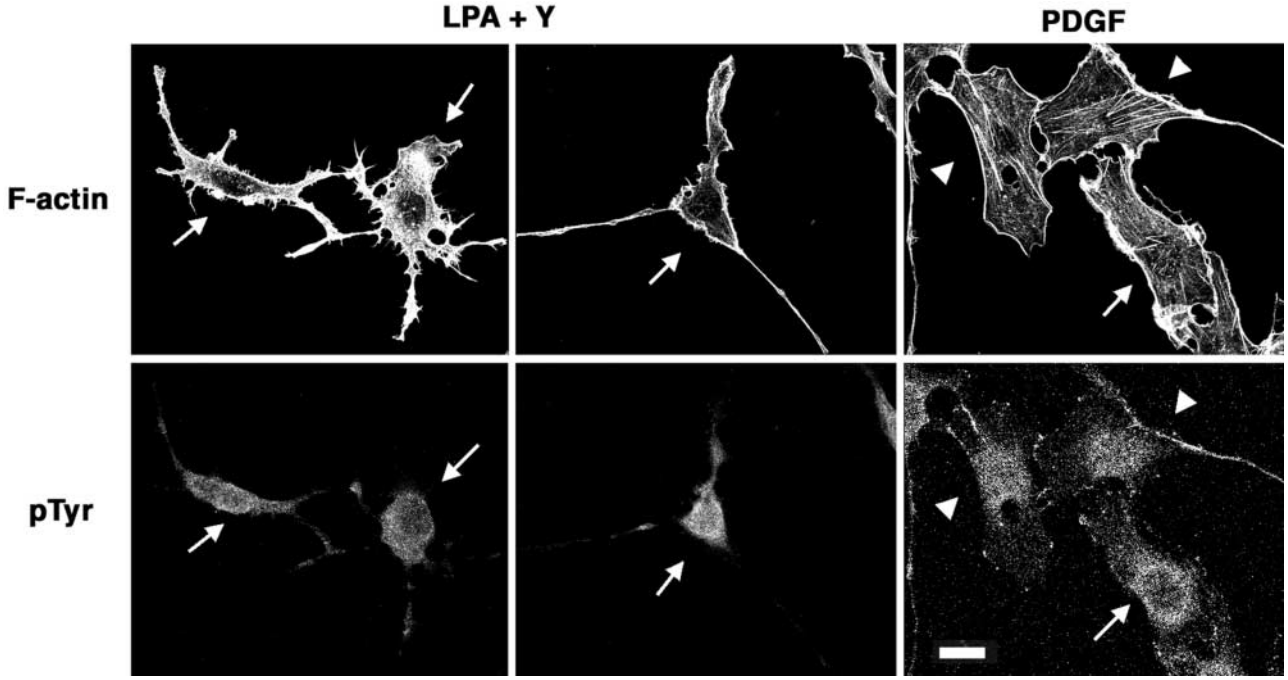

Figure 7. **Inhibition of LPA-induced membrane ruffles by expression of mDia1ΔN3(HindIII) in Y-27632–treated cells.** Swiss 3T3 cells were transfected with 1 μg of pEGFP plasmid encoding ΔN3(HindIII) and cultured as described in the legend to Fig. 2 A. The cells were treated with 30 μM Y-27632 for 30 min and then stimulated with 5 μM LPA for 5 min in the continued presence of Y-27632. Alternatively, the cells were stimulated with 5 ng/ml PDGF for 10 min without Y-27632 or LPA treatment. The cells were fixed, and F-actin and tyrosine-phosphorylated proteins were stained as described above. Left and middle panels show the cells stimulated with Y-27632 and LPA. The right panel shows cells stimulated with PDGF. Arrows indicate the cells expressing GFP–ΔN3–HindIII as identified by anti-GFP antibody staining. Arrowheads indicate nontransfected cells. Note that LPA-induced membrane ruffle formation is significantly suppressed by expression of mDia1–ΔN3(HindIII). Bar, 20 μm.

tants, H + P, F2, and mDia1ΔN3(HindIII) potently inhibited cell elongation and interfered with alignment of actin fibers and MTs induced by mDia1ΔN3 (Fig. 6, B and C). We then expressed these three mDia1 mutants individually in Swiss 3T3 cells and examined LPA-induced cell morphology in Y-27632–treated cells. Expression of mDia1ΔN3(HindIII) (Fig. 7) significantly inhibited LPA-induced membrane ruffling in Y-27632–treated cells. The dot-like focal complexes disappeared, and spreading was inhibited as seen in the cells expressing the Crk dominant negative mutants. This suppression was observed in 28 out of 30 cells expressing this construct. In contrast, the mDia1ΔN3(HindIII) expression did not inhibit the spreading and ruffle formation induced by PDGF. On the other hand, expression of either of the other two shorter mutants did not inhibit the LPA-induced membrane ruffle formation (unpublished data), suggesting that interference with endogenous mDia1 requires simultaneous blocking of various mDia1 domains. These results indicate that mDia1 works specifically as a switch of Rho activation to Rac activation.

Effects of MT disruption on Y-27632–induced membrane ruffling in serum-stimulated cells

Then, how does mDia1 mediate this action? We demonstrated that active mDia1 induces MT orientation to align actin fibers (Ishizaki et al., 2001). Kaverina et al. (1999) also suggested that MTs can promote cell protrusion by targeting focal adhesions and exerting relaxing effects. Therefore, we examined the effects of MT disruption by nocodazole on Y-27632–induced membrane ruffling. Because nocodazole treatment caused detachment of serum-starved cells from the dish, we added Y-27632 to cells cultured with serum and examined the effect of nocodazole. The addition of Y-27632 induced membrane ruffling also in serum-cultured cells, whereas the addition of nocodazole alone induced strong stress fibers as reported previously (Enomoto, 1996) (Fig. 8). On the other hand, combined addition of Y-27632 and nocodazole greatly attenuated stress fibers, indicating that Y-27632 sufficiently inhibited the ROCK activity also in these cells. Notably, this combined treatment also suppressed membrane ruffle formation, suggesting that membrane ruffle formation induced by Y-27632 depends on the activity of intact MTs. To test if disruption of microtubules could affect tyrosine phosphorylation of Cas, we analyzed tyrosine phosphorylation of Cas in control cells and cells treated with Y-27632 alone, nocodazole alone, or nocodazole and Y-27632. However, the Cas phosphorylation in these serum-maintained cells was low compared with the LPA-stimulated cells, and we could not detect any change in Cas phosphorylation among the groups of cells tested (unpublished data).

Discussion

ROCK and mDia1 antagonize in Rho-dependent Rac activation

In this study, by comparing the effects of C3 exoenzyme and Y-27632 on LPA-induced morphological change in serum-

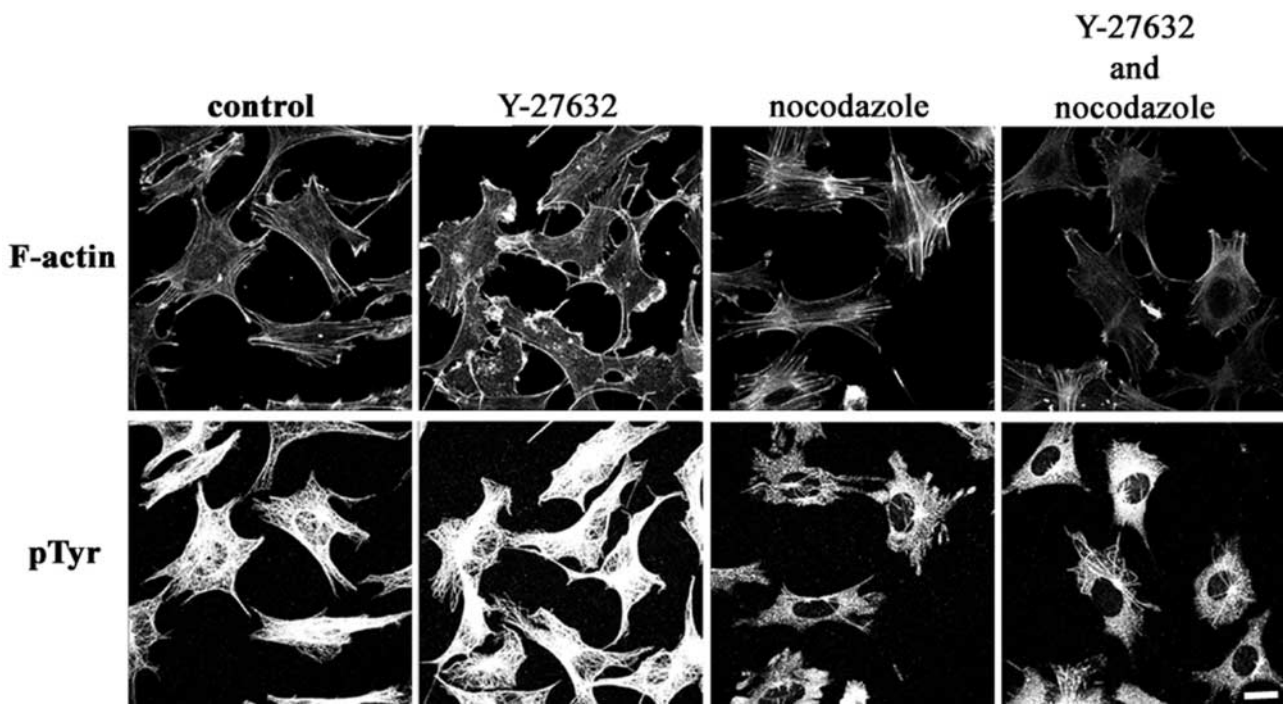

Figure 8. **Effects of nocodazole on Y-27632–induced membrane ruffles.** Swiss 3T3 cells were cultured in DME containing 10% FBS and treated with or without 30 μM Y-27632 in the presence or absence of 100 ng/ml nocodazole for 30 min. The cells were fixed and then stained for F-actin (top) and β-tubulin (bottom). Note that treatment of Y-27632 induced membrane ruffles at the tips of cells and that the addition of nocodazole inhibited the Y-27632–induced membrane ruffles. Bar, 20 μm.

starved Swiss 3T3 fibroblasts, we have first found that Rac is activated in a Rho-dependent manner, and this activation occurs when the ROCK pathway downstream of Rho is selectively inhibited. Induction of membrane ruffles by the Y-27632 treatment was reported previously by Rottner et al. (1999). These authors attributed this effect of ROCK inhibition to the presumed antagonism of Rho on Rac pathway originally observed in neuronal cells (Kozma et al., 1997; Van Leeuwen et al., 1997; Hirose et al., 1998). However, our findings that membrane ruffle formation and Rac activation were only seen in Y-27632–treated cells and not in cells treated with C3 exoenzyme argue against this hypothesis and suggest that a pathway mediated by other Rho effector(s) is responsible for this induction. Our subsequent analysis has indeed revealed that this Rac activation was evoked by the Rho-dependent tyrosine phosphorylation of Cas and the consequent formation of the Cas–Crk–DOCK180 complex. We have further found that the Y-27632–induced membrane ruffle formation was potently inhibited by expression of the dominant negative form of mDia1. mDia1 cooperates with ROCK downstream of Rho for correct induction of focal adhesions and stress fibers through MT alignment (Watanabe et al., 1999; Ishizaki et al., 2001). Binding of mDia1 to Src kinase and involvement of Src kinase in some mDia1-mediated actions was also reported (Tominaga et al., 2000). Src family kinases are also known to be responsible for integrin-dependent Cas phosphorylation (Klinghoffer et al., 1999). Consistently, the Y-27632–induced membrane ruffles in Swiss 3T3 cells were suppressed by disruption of MTs by nocodazole and inhibition of Src kinase by PP1. Together, these results suggest that mDia1 is an effector molecule mediating the Rho signal to Rac activation, and the ROCK pathway antagonizes this pathway of Rho-dependent Rac activation.

Then, how does the ROCK pathway antagonize the mDia1-mediated Rac activation? Because the level of GTP-Rac increases with ROCK inhibition (Fig. 2 B), the site of inhibition should be localized within the pathway from mDia1 to Rac activation by DOCK180. This inhibition site probably lies downstream of Cas because tyrosine phosphorylation of Cas was not enhanced by ROCK inhibition (Fig. 3, B and C). ROCK may interfere with this pathway through phosphorylation of paxillin. Yano et al. (2000) reported that paxillin α and Cas exert opposing effects on cell migration in a manner dependent on tyrosine phosphorylation of each protein. In this study, we have shown that tyrosine phosphorylation of paxillin is mediated by the ROCK pathway (Fig. 3, B and C).

Tyrosine phosphorylation of focal adhesion proteins occurs in many types of cells under a variety of stimuli, which utilize different signaling pathways. Therefore, our present findings naturally cannot be applied to every cell type. For example, in vascular endothelial cells stimulated with sphingosine-1 phosphate, tyrosine phosphorylation of Cas occurs in a manner not dependent on Rho (Ohmori et al., 2001), whereas similar to our finding bombesin induces Cas phosphorylation in a Rho-dependent, Y-27632–insensitive manner in Swiss 3T3 cells (Sinnett-Smith et al., 2001).

Implication of the dichotomy of the Rho signaling in the cell to substrate adhesion

The above findings suggest that two Rho effectors act differently downstream of Rho in the regulation of cell to sub-

strate adhesion and actin reorganization. Then, what is the implication of this dichotomy of the Rho signaling? The signaling and cytoskeletal dynamics that occur in cell spreading and adhesion as we analyzed in this study are generally thought to mimic events in migrating cells. Indeed, the bimodal Rho actions in migrating cells were suggested by an in vitro wound healing experiment using REF cells. Nobes and Hall (1999) microinjected two doses of C3 exoenzyme into migrating REF cells and found that the low dose that was sufficient to abolish stress fibers and focal adhesions did not affect cell migration, whereas the high dose completely inhibited cell migration. They also found that Y-27632 treatment accelerated the migration of the cells. The latter finding appears to be consistent with our current findings that treatment with Y-27632 and not C3 exoenzyme induces membrane ruffles. We have also found that treatment with Y-27632 and not C3 exoenzyme enhances the LPA-induced migration of Swiss 3T3 cells in the transwell assay (unpublished data). These results together with the above findings with the different doses of C3 exoenzyme suggest that the ROCK and mDia pathways differ in their sensitivities to C3 exoenzyme, the former being preferentially affected by the low dose and the latter becoming affected by the high dose. Such different sensitivities to C3 exoenzyme may indicate that activation of these two Rho pathways depend on the level of GTP-Rho in the cell, the low level being sufficient for the mDia1 pathway and the high level being required for the ROCK pathway. The level of GTP-Rho in the cell is regulated by both guanine nucleotide exchange factor and GTPase-activating protein (GAP) selective to this GTPase. Recently, Arthur and Burridge (2001) reported that the overexpression of wild-type p190RhoGAP facilitates spreading and migration of fibroblasts, whereas that of dominant negative p190RhoGAP (RA) inhibits these processes and that these phenotypes correlated with the low and high GTP-Rho levels, respectively. The phenotype induced by wild-type p190RhoGAP are similar to those of Y-27632–treated cells we described here, suggesting that p190RhoGAP may decrease the GTP-Rho level to interfere with the ROCK pathway. Consistently, they reported that the phenotype induced by the dominant negative p190RhoGAP (RA) mutant was reversed by the low dose of C3 exoenzyme. These results are consistent with a widely held view that the basal Rho activity is essential for cell migration and spreading (Nobes and Hall, 1999; Arthur and Burridge, 2001). Interestingly, the activity of p190RhoGAP is regulated through phosphorylation by c-Src that is activated in an integrin-dependent manner (Arthur et al., 2000). mDia1 may mediate this recruitment of Src to focal adhesions.

The dichotomy of the Rho signaling in the cell to substrate adhesion may also be important in the regulation of the cell cycle by Rho. The G1 to S phase progression of Swiss 3T3 cells is inhibited by C3 exoenzyme but not by Y-27632 (Yamamoto et al., 1993; Ishizaki et al., 2000). It is interesting to examine whether the mDia1-mediated signaling we described here works in this process. Another process where the mDia1-mediated signaling may work is Ras-induced cell transformation. Although Rho signaling is essential in Ras-induced transformation (Qiu et al., 1995), neither stress fibers nor focal adhesions are found in Ras-transformed cells, indicating that the Rho signaling is somehow modified in these cells. Sahai et al. (2001) reported that ROCK is down-regulated by both decreased expression and the cytoskeletal sequestration, whereas the level of GTP-Rho is elevated in Ras-transformed cells. These results indicate that the Rho signaling other than the ROCK pathway is important in the Ras-induced malignant transformation.

Rho-dependent Rac activation and the spatiotemporal control of cell migration

Cell migration is presumably performed by concerted formation of filopodia, lamellipodia, and actomyosin contraction each induced by the Rho family GTPases, Cdc42, Rac, and Rho (Mitchison and Cramer, 1996). Previously, the hierarchical activation of Cdc42 to Rac and then to Rho was shown and suggested to work in a cascade in cell migration (Chant and Stowers, 1995). However, these studies did not provide any information on activation of Rac or Cdc42 by Rho, which is essential to resume the migration cycle. Our present findings have for the first time demonstrated that the Rho signaling has a built-in switch for Rac activation. We have found that this switch is mediated by mDia1 and inhibited by ROCK. In this respect, it is interesting that mDia1 recruits MT ends to focal adhesions (Ishizaki et al., 2001) and that targeting of focal adhesions by MTs appears to inhibit the ROCK activity there (Kaverina et al., 1999). Together, these results suggest that the Rho-dependent Rac activation may be switched on in a positive feedback manner by mDia1. In migrating cells, signaling pathways of these Rho GTPases are regulated not only temporally but also spatially. mDia1 was previously shown to be localized in membrane ruffles of motile cells (Watanabe et al., 1997). On the other hand, recent studies suggest that the ROCK activity is required in the tail retraction of migrating monocytes and neutrophils (Worthylake et al., 2001). Thus, the two Rho signaling pathways may operate differently in space in migrating cells, the mDia1 and ROCK pathways preferentially in the front and the rear, respectively.

Materials and methods

Materials

LPA, nocodazole, anti-FLAG monoclonal antibody (M2), and anti–β-tubulin antibody (TUB.2.1) were purchased from Sigma-Aldrich. Antiphosphotyrosine polyclonal antibody (PY20) and monoclonal antibody (4G10) were purchased from Zymed Laboratories and Upstate Biotechnology, respectively. Clone 2A7 and clone 77 anti-FAK monoclonal antibodies were purchased from Upstate Biotechnology and Transduction Laboratory, respectively. Antipaxillin monoclonal antibody was purchased from Zymed Laboratories. PDGF-BB, anti-Rac1, and anti-Crk antibodies were purchased from Upstate Biotechnology. Anti-p130Cas polyclonal antibody was reported previously (Nakamoto et al., 1997). Y-27632, a ROCK inhibitor, was supplied by Mitsubishi Pharma. *Botulinum* C3 exoenzyme was purified as described (Morii and Narumiya, 1995). GST-PAK CRIB protein was prepared as described previously (Matsuo et al., 2002).

Plasmids

pE–green fluorescent protein (GFP)–C1 was purchased from CLONTECH Laboratories, Inc. pSSRα–p130CasΔSD, pEEB–CrkII(R38K), and pEEB–CrkII(W170K) were described previously (Nakamoto et al., 1997; Albert et al., 2000). pFL–mDia1ΔN3, pEGFP–mDia1–F2, and pEGFP–mDia1–H + P were constructed as described previously (Watanabe et al., 1999; Ishizaki et al., 2001). For construction of pEGFP–mDia1–CC, PCR was performed with

pFL–mDia1–Full (Watanabe et al., 1999) as a template using a forward primer (5′-TTCCTCGAGGCCTTCGGCCTCGCCTC-3′) and a reverse primer (5′-TTCGGATCCGTCCATCACACCTGTCTCATC-3′). The product was digested with XhoI and BamHI and inserted into a XhoI-BamHI fragment of pEGFP–C1. For construction of pEGFP–mDia1ΔN3(HindIII), pGEX–4T–mDia1ΔN3 was digested with BglII and HindIII. The insert was ligated with a BglII-HindIII fragment of pEGFP–C1. pCMV5–FLAG–N19Rac was described previously (Hirose et al., 1998). pEGFP actin was constructed as follows. Mouse β-actin cDNA was amplified from adult mouse brain mRNA using reverse transcriptase–PCR. NcoI-FSPI fragment was inserted between Asp718I and BamHI sites in pEGFP–C1 with the blunt-end ligation. The resultant plasmid contains mouse β-actin ORF fused to the COOH terminus of EGFP in frame with the linker of 17 amino acids.

Cell culture and transfection

For LPA stimulation of nontransfected cells, Swiss 3T3 cells were plated at densities of 2×10^4 and 2×10^5 cells per 35- and 60-mm dish for immunofluorescence study or immunoprecipitation assay, respectively, and cultured in DME containing 10% FCS for 3 d. The cells were washed twice with Ca^{2+}- and Mg^{2+}-free PBS(−) and cultured in serum-free DME for 24 h. During this period, the cells were without treatment or treated either with 30 μg/ml C3 exoenzyme all through the culture of 4 d or with 30 μM Y-27632 for the last 30 min. The cells were then stimulated with 5 μM LPA for the indicated times in the continued presence of C3 coenzyme or Y-27632. The cells were either fixed or lysed as described below. For transfection, Swiss 3T3 cells were plated on a cover glass at a density of 2×10^4 cells per 22-mm dish and cultured in DME containing 10% FCS for 24 h. The cells were washed with PBS(−) once and incubated with the indicated amounts of plasmid DNA(s) mixed with 1 μl of Lipofectamine 2000 for 3 h in 1 ml of OPTI-MEM (GIBCO BRL). The medium was replaced with DME containing 10% FCS, and the cells were cultured for 18 h. The cells were then cultured in serum-free DME for 24 h and treated with Y-27632 for the last 30 min. The cells were stimulated with 5 μM LPA for the indicated times in the continued presence of Y-27632. The cells were fixed and stained as described below. As indicated, PDGF stimulation on nontransfected or transfected cells was performed at 5 ng/ml concentration for 10 min.

HeLa cells were plated on a cover glass at a density of 5×10^4 cells per 35-mm dish and cultured in DME containing 10% FCS for 24 h. The cells were washed once and incubated with 0.2 μg of pFL–mDia1ΔN3 with or without 2 μg of the pEGFP plasmid encoding each mDia1 mutant mixed with 4 μl of Lipofectamine (GIBCO BRL) for 3 h in 1 ml of OPTI-MEM (GIBCO BRL). The medium was replaced with DME containing 10% FCS, and the cells were cultured for 18 h. The cells were then fixed and stained.

Immunofluorescence study

The cells were washed once with PBS(−) and fixed as follows. HeLa cells were fixed with 4% formaldehyde as described previously (Ishizaki et al., 2001). Swiss 3T3 cells were fixed first for 1 min with 4% formaldehyde and 0.1% Triton X-100 in PBS and then for 15 min with 4% formaldehyde alone in PBS. Both lines of the cells were permeabilized by washing in PBS(−) containing 0.1% Triton X-100 for 5 min and incubated with PBS(−) containing 3% BSA for 1 h at room temperature. Primary antibodies were diluted in PBS(−) containing 1% BSA and included the antibodies against pTyr (1:100), β-tubulin (1: 200), the Flag tag (1:100), and the GFP tag (1:100). F-actin was always stained with Texas red phalloidin (Molecular Probes). In double staining for F-actin and phosphotyrosine, Alexa Fluor 488–conjugated goat anti–mouse IgG (H + L) (Molecular Probes) was used as the secondary antibody. In triple staining for F-actin, phosphotyrosine, and tag epitopes, Alexa Fluor 488–conjugated goat anti–mouse IgG (H + L) was used for detection of the signal of the tag epitope, and Alexa Fluor 633–conjugated goat anti–rabbit IgG (H + L) (Molecular Probes) was used for detection of the signal of rabbit polyclonal antibody to phosphotyrosine. Alexa Fluor 594–conjugated goat anti–rabbit IgG (H + L) (Molecular Probes) was used as the secondary antibody for detection of MTs. Optical sections of 0.3-μm thickness were obtained from the bottom with a Bio-Rad Laboratories MRC1024 Confocal Imaging System, and built-up images were constructed.

Videomicroscopy

Swiss 3T3 cells were seeded at a density of 2×10^4 per dish in a 35-mm glass-bottom dish (Matsunami Glass) and cultured for 24 h. The cells were transfected with 1 μg of pEGFP actin as described above and then maintained for 3 d. The cells were starved in serum-free DME for 24 h and treated with 30 μM Y-27632 for the last 30 min. The dish was transferred to a temperature-controlled ZEISS CO_2 incubator attached to the microscope stage. 5 μM LPA was then added, and the cell movement was monitored at 37°C in 5% CO_2 for 90 min using a ZEISS confocal laser scanning unit (LSM 510-V2.5). Three successive optical sections of 0.6-μm thickness were obtained from the bottom every 90 s, and built-up images were constructed.

Western blot analysis and immunoprecipitation

Swiss 3T3 cells were washed once with ice-cold PBS(−) and lysed on ice for 5 min with modified RIPA buffer containing 50 mM Tris-HCl, pH 7.5, 150 mM NaCl, 1% NP-40, 0.25% SDS, 0.25% sodium deoxycholate, 1 mM sodium fluoride, 1 mM sodium orthovanadate, 1 μg/ml leupeptin, 1 μg/ml aprotinin, 1 μg/ml pepstatin, 1 mM EGTA, and 1 mM PMSF. The samples were centrifuged at 12,000 *g* for 20 min, and the supernatant was collected as the cell lysates. Protein concentration of the lysates was determined by the Lowry method. For Western blot analysis using the total cell lysates, one fifth volume of the 5× Laemmli sample buffer was added to the lysates. The mixtures were boiled for 5 min and subjected to SDS-PAGE and Western blot analysis using antiphosphotyrosine antibody (4G10) as described (Needham and Rozengurt, 1998). For immunoprecipitation, 50 μg of each cell lysate was incubated with 1 μg of either anti-p130Cas polyclonal antibody, anti-FAK monoclonal antibody, antipaxillin monoclonal antibody, or antiphosphotyrosine monoclonal antibody (4G10). 30 μl of either protein A–Sepharose (for precipitation of anti-p130Cas antibody complex only) or protein G–Sepharose (Amasham Pharmacia Biotech) were then added, and incubation was performed for 3 h at 4°C. The Sepharose beads were washed three times with the lysis buffer and suspended with an equal volume of 2× Laemmli sample buffer. The suspensions were boiled, and the extracts were subjected to Western blot analysis using the indicated antibodies. Immunoprecipitation of Crk was performed as described (Gu et al., 2001).

Pull-down assay

Swiss 3T3 cells were plated at a density of 5×10^5 cells per 10-cm dish. Culture, treatment with Y-27632, or C3 exoenzyme and LPA stimulation were performed as described above. The cells were washed once with ice-cold PBS(−) and lysed in the pull-down lysis buffer containing 50 mM Tris-HCl, pH 7.5, 100 mM NaCl, 2 mM $MgCl_2$, 10% glycerol, 1% NP-40, 1 μg/ml leupeptin, 1 μg/ml aprotinin, 1 μg/ml pepstatin, 1 mM sodium fluoride, 1 mM EGTA, and 1 mM PMSF. The samples were centrifuged at 12,000 *g* for 20 min, and the supernatants were saved as the cell lysates. After protein concentration was determined by the Lowry method, 200 μg protein of cell lysate was incubated with 20 μg protein of GST-PAK CRIB immobilized on glutathione–Sepharose 4B beads (Amersham Pharmacia Biotech) for 1 h at 4°C. Beads were washed three times with the pull-down buffer, and bound GTP-Rac1 was detected by Western blot with anti-Rac1 antibody.

Online supplemental materials

Fig. S1, showing the effect of Y-27632 on morphology of C3 exoenzyme-treated cells, Fig. S2, showing the effect of PDGF on morphology of C3 exoenzyme-treated cells, and the video, showing LPA-induced membrane ruffling of Y-27632–treated cells, are available online at http://www.jcb.org/cgi/content/full/jcb.200112107/DC1.

We thank Dr. M. Hoshino for providing pGEX–PAK–CRIB, Dr. H. Bito for useful advice, and Ms. K. Nonomura, H. Nose, and T. Arai for assistance.

This work was supported in part by a grant in aid for Specially Promoted Research from the Ministry of Education, Culture, Sports Science and Technology of Japan and a grant from the Organization for Pharmaceutical Safety and Research.

Submitted: 20 December 2001
Revised: 12 April 2002
Accepted: 12 April 2002

References

Albert, M.L., J.I. Kim, and R.B. Birge. 2000. $\alpha_v\beta_5$ integrin recruits the CrkII-Dock180-rac1 complex for phagocytosis of apoptotic cells. *Nat. Cell Biol.* 2:899–905.

Allen, W.E., D. Zicha, A.J. Ridly, and G.E. Jones. 1998. A role for Cdc42 in macrophage chemotaxis. *J. Cell Biol.* 141:1147–1157.

Amano, M., K. Chihara, K. Kimura, Y. Fukata, N. Nakamura, Y. Matsuura, and K. Kaibuchi. 1997. Formation of actin stress fibers and focal adhesions enhanced by Rho-kinase. *Science.* 275:1308–1311.

Arthur, W.T., and K. Burridge. 2001. RhoA inactivation by p190RhoGAP regulates cell spreading and migration by promoting membrane protrusion and polarity. *Mol. Biol. Cell.* 12:2711–2720.

Arthur, W.T., L.A. Petch, and K. Burridge. 2000. Integrin engagement suppresses RhoA activity via a c-Src-dependent mechanism. *Curr. Biol.* 10:719–722.

Chant, J., and L. Stowers. 1995. GTPase cascades choreographing cellular behavior: movement, morphogenesis, and more. *Cell.* 81:1–4.

Enomoto, T. 1996. MT disruption induces the formation of actin stress fibers and focal adhesions in cultured cells: possible involvement of the Rho signal cascade. *Cell Struct. Funct.* 21:317–326.

Gu, J., Y. Sumida, N. Sanzen, and K. Sekiguchi. 2001. Laminin-10/11 and fibronectin differentially regulate integrin-dependent Rho and Rac activation via $p130^{Cas}$-CrkII-DOCK180 pathway. *J. Biol. Chem.* 276:27090–27097.

Hall, A. 1998. Rho GTPases and the actin cytoskeleton. *Science.* 279:509–514.

Hanke, J.H., J.P. Gardner, R.L. Dow, P.S. Changelian, W.H. Brissette, E.J. Weringer, B.A. Pollok, and P.A. Connelly. 1996. Discovery of a novel, potent, and Src family-selective tyrosine kinase inhibitor. Study of Lck- and Fyn-dependent T cell activation. *J. Biol. Chem.* 271:695–701.

Hirose, M., T. Ishizaki, N. Watanabe, M. Uehata, O. Kranenburg, W.H. Moolenaar, F. Matsumura, M. Maekawa, H. Bito, and S. Narumiya. 1998. Molecular dissection of the Rho-associated protein kinase (p160ROCK)-regulated neurite remodeling in neuroblastoma N1E-115 cells. *J. Cell Biol.* 141:1625–1636.

Horwitz, A.R., and J.T. Parsons. 1999. Cell migration—movin' on. *Science.* 286: 1102–1103.

Ishizaki, T., M. Naito, K. Fujisawa, M. Maekawa, N. Watanabe, Y. Saito, and S. Narumiya. 1997. p160ROCK, a Rho-associated coiled-coil forming protein kinase, works downstream of Rho and induces focal adhesions. *FEBS Lett.* 404:118–124.

Ishizaki, T., M. Uehata, I. Tamechika, J. Keel, K. Nonomura, M. Maekawa, and S. Narumiya. 2000. Pharmacological properties of Y-27632, a specific inhibitor of rho-associated kinases. *Mol. Pharmacol.* 57:976–983.

Ishizaki, T., Y. Morishima, M. Okamoto, T. Furuyashiki, T. Kato, and S. Narumiya. 2001. Coordination of MTs and the actin cytoskeleton by the Rho effector mDia1. *Nat. Cell Biol.* 3:8–14.

Kaverina, I., O. Krylyshkina, and J.V. Small. 1999. MT targeting of substrate contacts promotes their relaxation and dissociation. *J. Cell Biol.* 146:1033–1044.

Kiyokawa, E., Y. Hashimoto, S. Kobayashi, H. Sugimura, T. Kurata, and M. Matsuda. 1998. Activation of Rac1 by a Crk SH3-binding protein, DOCK180. *Genes Dev.* 12:3331–3336.

Klemke, R.L., J. Leng, R. Molander, P.C. Brooks, K. Vuori, and D.A. Cheresh. 1998. CAS/Crk coupling serves as a "molecular switch" for induction of cell migration. *J. Cell Biol.* 140:961–972.

Klinghoffer, R.A., C. Sachsenmaier, J.A. Cooper, and P. Soriano. 1999. Src family kinases are required for integrin but not PDGFR signal transduction. *EMBO J.* 18:2459–2471.

Kozma, R., S. Sarner, S. Ahmed, and L. Lim. 1997. Rho family GTPases and neuronal growth cone remodeling: relationship between increased complexity induced by Cdc42Hs, Rac1, and acetylcholine and collapse induced by RhoA and lysophosphatidic acid. *Mol. Cell. Biol.* 17:1201–1211.

Kumagai, N., N. Morii, K. Fujisawa, Y. Nemoto, and S. Narumiya. 1993. ADP-ribosylation of rho p21 inhibits lysophosphatidic acid-induced protein tyrosine phosphorylation and phosphatidylinositol 3-kinase activation in cultured Swiss 3T3 cells. *J. Biol. Chem.* 268:24535–24538.

Leung, T., X.Q. Chen, E. Manser, and L. Lim. 1996. The p160 RhoA-binding kinase ROK alpha is a member of a kinase family and is involved in the reorganization of the cytoskeleton. *Mol. Cell. Biol.* 16:5313–5327.

Matsuo, N., M. Hoshino, M. Yoshizawa, and Y. Nabeshima. 2002. Characterization of STEF, a guanine nucleotide exchange factor for Rac1, required for neurite growth. *J. Biol. Chem.* 277:2860–2868.

Mitchison, T.J., and L.P. Cramer. 1996. Actin-based cell motility and cell locomotion. *Cell.* 84:371–379.

Morii, N., and S. Narumiya. 1995. Preparation of native and recombinant *Clostridium botulinum* C3 ADP-ribosyltransferase and identification of Rho proteins by ADP-ribosylation. *Methods Enzymol.* 256:196–206.

Nakamoto, T., R. Sakai, H. Honda, S. Ogawa, H. Ueno, T. Suzuki, S. Aizawa, Y. Yazaki, and H. Hirai. 1997. Requirements for localization of p130cas to focal adhesions. *Mol. Cell. Biol.* 17:3884–3897.

Narumiya, S. 1996. The small GTPase Rho: cellular functions and signal transduction. *J. Biochem. (Tokyo).* 120:215–228.

Needham, L.K., and E. Rozengurt. 1998. Gα12 and Gα13 stimulate Rho-dependent tyrosine phosphorylation of focal adhesion kinase, paxilin, and p130 Crk-associated substrate. *J. Biol. Chem.* 273:14626–14632.

Nobes, C.D., and A. Hall. 1999. Rho GTPases control polarity, protrusion, and adhesion during cell movement. *J. Cell Biol.* 144:1235–1244.

Ohmori, T., Y. Yatomi, H. Okamoto, Y. Miura, G. Rile, K. Satoh, and Y. Ozaki. 2001. Gi-mediated Cas tyrosine phosphorylation in vascular endothelial cells stimulated with sphingosine 1-phosphate: possible involvement in cell motility enhancement in cooperation with Rho-mediated pathways. *J. Biol. Chem.* 276:5274–5280.

Okuda, M., M. Takahashi, J. Suehiro, C.E. Murry, O. Traub, H. Kawakatsu, and B.C. Berk. 1999. Shear stress stimulation of $p130^{cas}$ tyrosine phosphorylation requires calcium-dependent c-Src activation. *J. Biol. Chem.* 274:26801–26809.

O'Neill, GM., A.J. Fashena, and E.A. Golemis. 2000. Integrin signalling: a new Cas(t) of characters enters the stage. *Trends Cell Biol.* 10:111–119.

Qiu, R.G., J. Chen, F. McCormick, and M. Symons. 1995. A role for Rho in Ras transformation. *Proc. Natl. Acad. Sci. USA.* 92:11781–11785.

Rankin, S., N. Morii, S. Narumiya, and E. Rozengurt. 1994. Botulinum C3 exoenzyme blocks the tyrosine phosphorylation of p125FAK and paxillin induced by bombesin and endothelin. *FEBS Lett.* 354:315–319.

Ridley, A.J., and A. Hall. 1992. The small GTP-binding protein rho regulates the assembly and focal adhesions and actin stress fibers in response to growth factors. *Cell.* 70:389–399.

Rottner, K., A. Hall, and J.V. Small. 1999. Interplay between Rac and Rho in the control of substrate contact dynamics. *Curr. Biol.* 9:640–648.

Sahai, E., M.F. Olson, and C.J. Marshall. 2001. Cross-talk between Ras and Rho signalling pathways in transformation favours proliferation and increased motility. *EMBO J.* 20:755–766.

Sakai, R., A. Iwamatsu, N. Hirano, S. Ogawa, T. Tanaka, H. Mano, Y. Yazaki, and H. Hirai. 1994. A novel signaling molecule, p130, forms stable complexes in vivo with v-Crk and v-Src in a tyrosine phosphorylation-dependent manner. *EMBO J.* 13:3748–3756.

Sander, E.E., S. van Delft, J.P. ten Klooster, T. Reid, R.A. van der Kammen, F. Michiels, and J.G. Collard. 1998. Matrix-dependent Tiam1/Rac signaling in epithelial cells promotes either cell-cell adhesion or cell migration and is regulated by phosphatidylinositol 3-kinase. *J. Cell Biol.* 143:1385–1398.

Schmitz, A.A., E.E. Govek, B. Bottner, and L. Van Aelst. 2000. Rho GTPases: signaling, migration, and invasion. *Exp. Cell Res.* 261:1–12.

Sinnett-Smith, J., J.A. Lunn, D. Leopoldt, and E. Rozengurt. 2001. Y-27632, an inhibitor of Rho-associated kinases, prevents tyrosine phosphorylation of focal adhesion kinase and paxillin induced by bombesin: dissociation from tyrosine phosphorylation of $p130^{CAS}$. *Exp. Cell Res.* 266:292–302.

Tominaga, T., E. Sahai, P. Chardin, F. McCormick, S.A. Courtneidge, and A.S. Alberts. 2000. Diaphanous-related formins bridge Rho GTPase and Src tyrosine kinase signaling. *Mol. Cell.* 5:13–25.

Uehata, M., T. Ishizaki, H. Satoh, T. Ono, T. Kawahara, T. Morishita, H. Tamakawa, K. Yamagami, J. Inui, M. Maekawa, and S. Narumiya. 1997. Calcium sensitization of smooth muscle mediated by a Rho-associated protein kinase in hypertension. *Nature.* 389:990–994.

Van Leeuwen, F.N., H.E.T. Kain, R.A. van de Kammen, F. Michiels, O.W. Kranenburg, and J.C. Collard. 1997. The guanine nucleotide exchange factor Tiam 1 affects neuronal morphology: opposing roles for the small GTPases Rac and Rho. *J. Cell Biol.* 139:797–807.

Watanabe, N., P. Madaule, T. Reid, T. Ishizaki, G. Watanabe, A. Kakizuka, Y. Saito, K. Nakao, B.M. Jockusch, and S. Narumiya. 1997. p140mDia, a mammalian homolog of *Drosophila diaphanous*, is a target protein for Rho small GTPase and is a ligand for profilin. *EMBO J.* 16:3044–3056.

Watanabe, N., T. Kato, A. Fujita, T. Ishizaki, and S. Narumiya. 1999. Cooperation between mDia1 and ROCK in Rho-induced actin reorganization. *Nat. Cell Biol.* 1:136–143.

Worthylake, R.A., S. Lemoine, J.M. Watson, and K. Burridge. 2001. RhoA is required for monocyte tail retraction during transendothelial migration. *J. Cell Biol.* 154:147–160.

Yamamoto, M., N. Marui, T. Sakai, N. Morii, S. Kozaki, K. Ikai, S. Imamura, and S. Narumiya. 1993. ADP-ribosylation of the rhoA gene product by botulinum C3 exoenzyme causes Swiss 3T3 cells to accumulate in the G1 phase of the cell cycle. *Oncogene.* 8:1449–1455.

Yano, H., H. Uchida, T. Iwasaki, M. Mukai, H. Akedo, K. Nakamura, S. Hashimoto, and H. Sabe. 2000. Paxillin α and Crk-associated substrate exert opposing effects on cell migration and contact inhibition of growth through tyrosine phosphorylation. *Proc. Natl. Acad. Sci. USA.* 97:9076–9081.